JMEPEG (2005) 14:623-633
DOI: 10.1361/105994905X64503

1059-9495/$19.00

Identification of Heat Treatments for Better Formability in an Aluminum-Lithium Alloy Sheet

M.L. Bairwa, Sharvari G. Desai, and P.P. Date

(Submitted November 29, 2004; in revised form April 1, 2005)

Research in the weight of an automobile is a continuous process among auto manufacturers. The "body in white" (BIW, i.e., the body of the car) deserves attention, being a major contributor to the weight of the vehicle. By virtue of a high strength to weight ratio (density smaller than aluminum) and a higher Young's modulus than aluminum, aluminum-lithium alloy sheet appears to hold promise as an autobody material. Because auto components are required in large numbers and are formed at room temperature, formability under these conditions becomes significant. Aluminum-lithium alloys acquire, because of aging over a short period of time, a good amount of strength and hence dent resistance. In principle, they can be given, through suitable heat treatments, a high formability as well as dent resistance, i.e., an ideal combination of properties. To this end, tensile properties have been determined for a number of heat treatments comprising three different solutionizing temperatures and for three aging times at each of the three aging temperatures. Considerable influence of heat treatment was observed on the mechanical properties (which in turn characterize both formability and dent resistance), such as the strain hardening exponent, average normal anisotropy, yield stress, ultimate tensile stress, and percentage elongation to failure. For each property, the best three heat treatments leading to a high formability were identified. Consequently, heat treatments that imparted the greatest formability for processes such as deep drawing and stretch forming have been identified. The investigations show that the best heat treatment for one property may not be the best for another property, calling for a compromise to obtain the most practicable heat treatment schedule. Results shed light on not only the biaxial formability but also springback behavior that is important in the BIW components. Further, the properties obtained from the heat treatment giving good formability in deep drawing were used to simulate car body fender and the S-rail using sheet metal forming simulation software PAMSTAMP2G. A comparison of simulation of aluminum-lithium alloy fender and S-rail with those made from steel demonstrates advantages using aluminum-lithium alloys in terms of weight reduction. Finally, based on the current oil prices and the projected demand for oil in the next decade, aluminum-lithium alloys seem to have an edge despite the difficulties in manufacturing, assembly, and joining of the aluminum-lithium components.

Keywords aluminum-lithium alloys, formability, heat treatments, tensile properties

1. Introduction

From an environmental point of view, fuel-efficient vehicles that also have lower emission of CO_2 in the exhaust are being developed. The developments include improvements in the thermal efficiency of the engine; reduction of the weight of the engine, the drives, the suspensions, and the body in white (BIW, i.e., the body of the car); and reduction in the aerodynamic drag (Ref 1-7). One effective method of reducing fuel consumption is reduction in the weight of the BIW. Body manufacturing technologies contribute around 35% toward fuel economy (Ref 1). For this reason, autobody materials (such as high-strength, low-alloy steels and aluminum alloys) would be expected to play a significant role in the future generation of cars.

The concept of an aluminum autobody has been in vogue for more than a decade. Aluminum-lithium alloys have low density and good mechanical properties such as moderate to high strength, relatively poor weldability, and good elevated temperature and cryogenic mechanical properties, but inferior resistance to pitting corrosion. Their amenability to superplastic forming makes aluminum-lithium alloys the first choice for many structural applications in the aerospace industry. This method may be used to cut down on the number of stages required to form some automobile parts. However, the quantity of automotive parts required is large, and superplastic forming or high-temperature processing might not be suitable. A study of aluminum as the most likely material is presented with pros and cons associated with manufacturability of aluminum over advantages associated with material properties (Ref 2).

Moreover, because aluminum-lithium alloys are costly, one wonders whether they can really be used for autobody parts where the cost of manufacture is a concern. It is therefore important to ensure adequate ductility at room temperature, under conditions in which the autobody parts are made on the shop floor. A comparison of high-strength, low-alloy steels with aluminum alloys based on mechanical behavior and their application to load-bearing body components of lightweight passenger vehicles was presented by Wilson (Ref 3). He highlighted limitations of the application of the aluminum alloy sheet compared with the steel sheet. Based on research on the projected population growth, the number of cars that will be

M.L. Bairwa, Sharvari G. Desai, and **P.P. Date,** Department of Mechanical Engineering, IIT Bombay, Powai, Mumbai 400076, India. Contact e-mail: ppdate@me.iitb.ac.in.

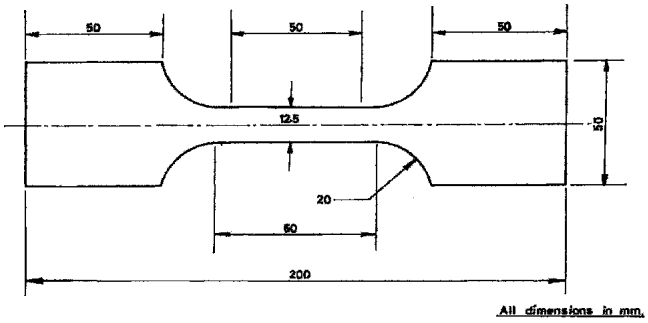

Fig. 1 Tensile testing specimen

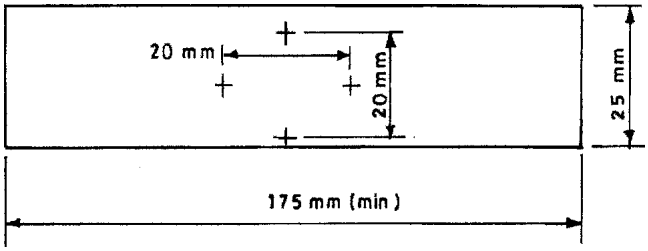

Fig. 2 *R*-value testing specimen (C-type)

required, and the rising demand for fuel, the prices of fuel can be expected to grow in the next two decades (Ref 4, 5). Fuel efficiency therefore will be mandatory in years to come (Ref 6, 7). Taking this into consideration and the relatively high cost of aluminum-lithium alloy sheets, automobiles might be a little expensive at the outset, but savings on the recurring cost of fuel could offset the high initial expense. A brief account of the likely savings based on weight reduction using aluminum-lithium alloy sheets alone is therefore given at the end of this paper.

Considerable work has been reported on aluminum-lithium alloys pertaining to formability, including the effect of chemical composition and the microstructure on the deformation behavior (characterized by the tensile properties). The tensile properties at different orientations with respect to the rolling direction (RD) have been studied (Ref 8). The effect of tempering (Ref 9) and different heat treatments (Ref 10-12) is reported in this study. Studies on aging treatments (Ref 13) and precipitation (Ref 14) called for different combinations of solutionizing temperature, aging temperature, and aging time. The effect of heat treatments on tensile properties (Ref 15) and their relevance to the forming process was studied using the analytical hierarchical process (AHP). In the present work the weighted performance index was determined for each of the 10 selected heat treatments. The best heat treatments were identified on this basis for drawing and stretching operations. Furthermore, these properties were used in the simulation of the forming process for an autobody fender and the S-rail (a structural member) using finite element sheet metal forming simulation software PAMSTAMP2G.

Some estimates on cost savings by virtue of weight reduction are presented at the end of the paper. The projected cost savings appear more promising than what they are likely to be because the rise in the cost of manufacture could not be considered as data on this aspect were not available to the authors.

2. Experimental Procedures

2.1 Material and Heat Treatments

The material used for this work was a 1.0 mm thick aluminum-lithium 1441-alloy sheet supplied by the sponsors. Tensile test specimens, as shown in Fig. 1, were prepared from the sheets in three directions, 0, 45, and 90 degrees to the RD. Specimens were then heat treated at the specified solutionizing temperature for about 40 min, quenched, and aged at the corresponding aging temperature for the aging time as determined from the factorial design of experiments. The values of the aging temperature, aging times, and solutionizing temperatures are:

- Aging temperatures of –17 °C, room temperature (RT), and 170 °C.
- Aging times of 1, 8, and 24 h at each of the aging temperatures
- Solutionizing temperatures of 520, 535, and 550 °C for 40 min

This led to 27 heat treatment combinations. In this work, a heat treatment is represented in the format: solutionizing temperature/aging temperature/aging time. Hence, a treatment of 550/170/1 would mean solutionizing temperature of 550 °C, an aging temperature of 170 °C, and an aging time of 1 h. The heat-treated tensile samples were pulled to failure and the load-extension data obtained for each of these treatments.

2.2 Tensile Tests

Heat-treated sheet specimens with a gauge length of 50 mm, oriented at 0, 45, and 90 degrees to the RD were tested on a SHIMADZU AG-5000G computer-controlled tensile testing machine. At least two specimens were tested in each of the three orientations with respect to RD at each of the 27 heat treatments (total number of specimens was thus $27 \times 3 \times 2 = 162$). Values of the strain hardening exponent (n) and K were determined using the standard ASTM E646 procedure (Ref 9) for each of the samples tested.

2.3 R-Value (Plastic Strain Ratio) Tests

The R-value was determined by pulling in uniaxial tension a C-type specimen (Fig. 2) recommended by ASTM E517 (1987) (Ref 10) specifications using a SHIMADZU AG-5000G computer-controlled tensile testing machine. The conditions under which the tests were conducted were the same as those for the tensile tests.

At the desired strain the test was stopped and the sample unloaded for measurements of strains in the gauge section. The R-values were measured at around 25% engineering strain in the gauge section using a NIKON Measurescope MM-22 (Japan) with a least count of 0.001 and 30× magnification.

Accuracy in R-value determination was ensured by using a NIKON Measurescope having least count of 0.001 and digital read out because accuracy in R-value measurements significantly depends on the measurements of the gauge dimensions.

3. Results

From the tensile tests, mechanical properties n, average normal anisotropy (R), yield stress (YS), ultimate tensile stress

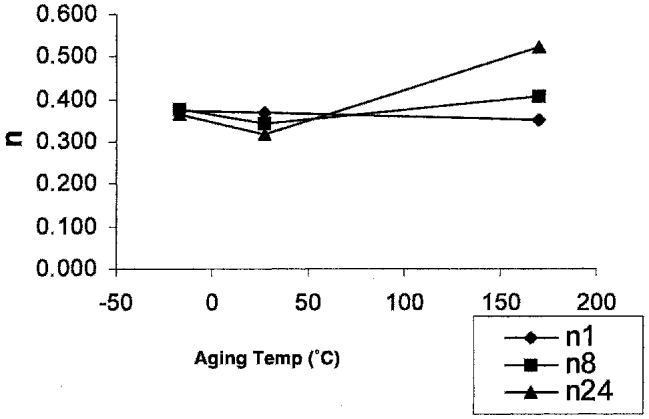

Fig. 3 Effect of aging temperature and time on *n* in RD. Solutionizing temperature 520 °C

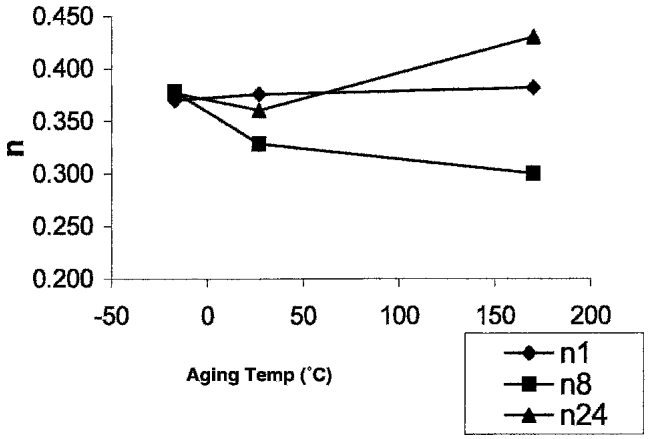

Fig. 4 Effect of aging temperature and time on *n* at 45 degrees to the RD. Solutionizing temperature 550 °C

(UTS), and percentage elongation to failure were calculated. Heat treatments that gave maximum formability based on each of the indices mentioned above were identified as described below.

3.1 Strain Hardening Exponent

The *n* value, which indicates the ability of the material to distribute the strain uniformly prior to diffuse necking, was calculated for all heat treatments. A material with a higher value of *n* shows greater uniform strain and hence greater formability. This was found to be maximum for heat treatment 520/170/24. Figures 3 to 5 are representations of maximum values of *n* for the best three treatments with different aging temperatures and aging times. Figure 6 shows the comparison between values of *n* for the best three conditions along the three directions with respect to the RD, and Fig. 7 is a similar comparison based on the average value of *n*.

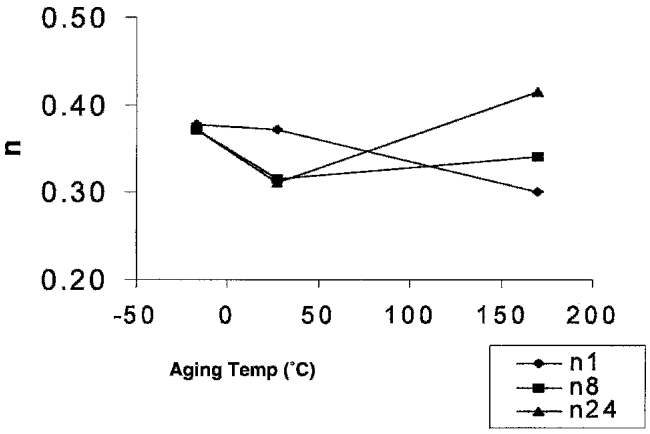

Fig. 5 Effect of aging temperature and time on *n* at 45 degrees to the RD. Solutionizing temperature 535 °C

3.2 Yield Strength

The effect of heat treatment on the YS, which characterizes the onset of plastic deformation of a material, was studied. Because a lower value of YS gives greater formability, heat treatment 535/RT/1 was found to be the best condition. Figures 8 to 10 represent minimum values of YS for best three heat treatments with different aging temperatures and aging times. Figure 11 shows a comparison of YS values for the best three conditions along the three directions with respect to RD. Figure 12 is a similar comparison based on the average value of YS.

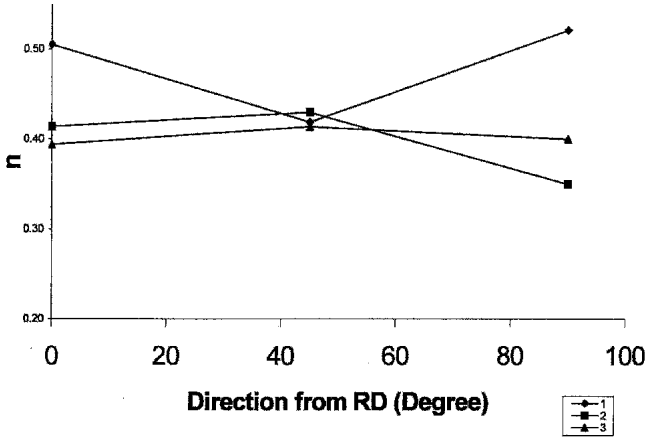

Fig. 6 Variation of *n* with respect to three RD values for the best three treatments (1 = 520/170/24, 2 = 550/170/24, 3 = 535/170/24)

3.3 Percentage Elongation

Percentage elongation, which is the total elongation up to failure, was studied because a greater percentage elongation would be expected to lead to greater formability. (We acknowledge at this point that the percentage elongation is not a reliable index of formability. However, because it is recommended by many standards, we report it in this paper.)

The treatment 535/–17/24 was found to be the best condition because it gives the maximum elongation to failure. Figures 13 to 15 represent the maximum values of elongation to failure for the best three heat treatments with different aging temperatures and times. Figure 16 is a comparison of the values of percentage elongation for the best three conditions along different directions with respect to the RD. Similarly, Fig. 17 is a comparison based on the average value of percentage elongation.

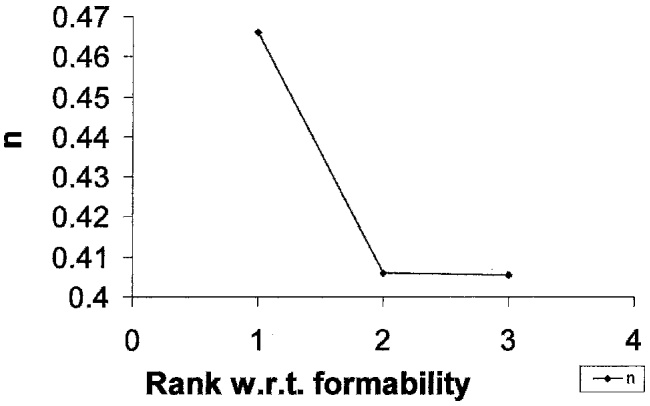

Fig. 7 Relative variation of *n* for the best three heat treatments based on a high *n* value (1 = 520/170/24, 2 = 550/170/24, 3 = 535/170/24)

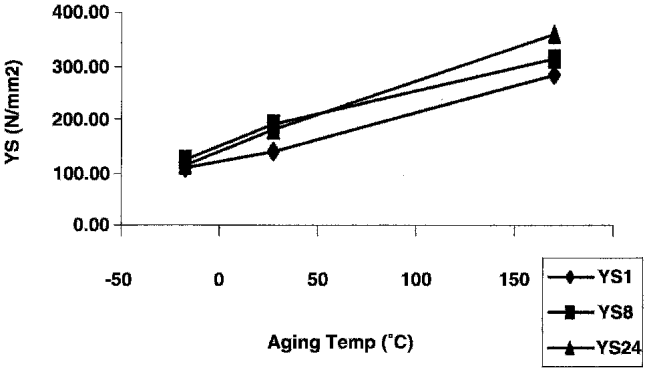

Fig. 8 Effect of aging temperature and time on YS at 90 degrees to the RD. Solutionizing temperature 550 °C

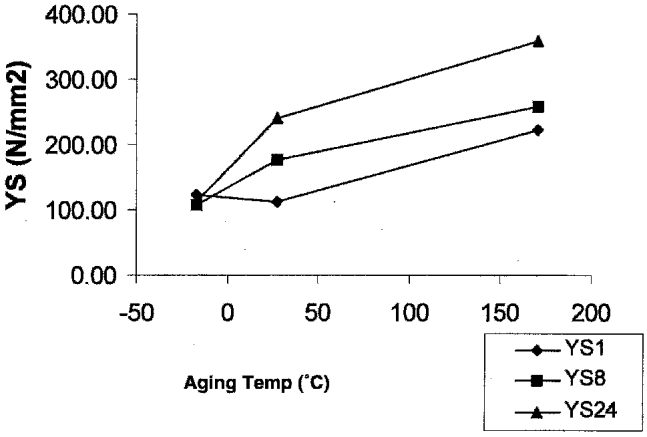

Fig. 9 Effect of aging temperature and time on YS at 45 degrees to the RD. Solutionizing temperature 550 °C

3.4 Ultimate Tensile Strength

A high value of UTS is desirable for formability. The treatment 550/170/24 was found to be most suitable from this viewpoint. Figures 18 to 20 represent the maximum values of UTS for the best three heat treatments. Figure 21 shows a comparison of UTS values for the best three conditions. Figure 22 compares the same based on the average value.

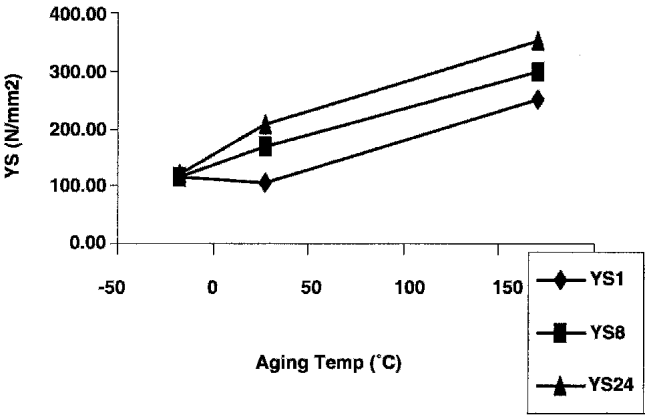

Fig. 10 Effect of aging temperature and time on YS at 45 degrees to the RD. Solutionizing temperature 535 °C

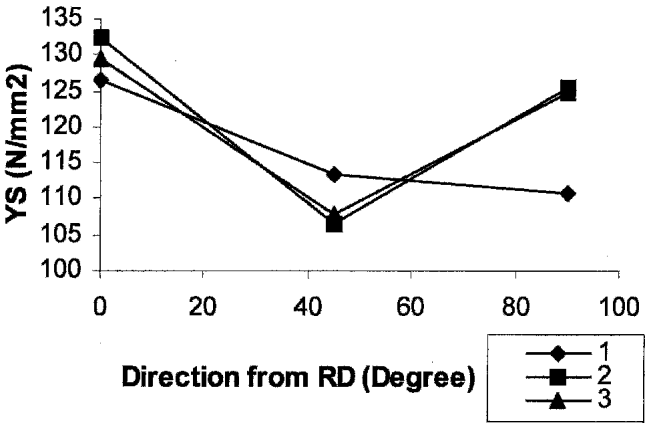

Fig. 11 Variation of YS with angle with respect to the RD for the best three treatments (1 = 550/–17/24, 2 = 550/-17/8, 3 = 535/RT/1)

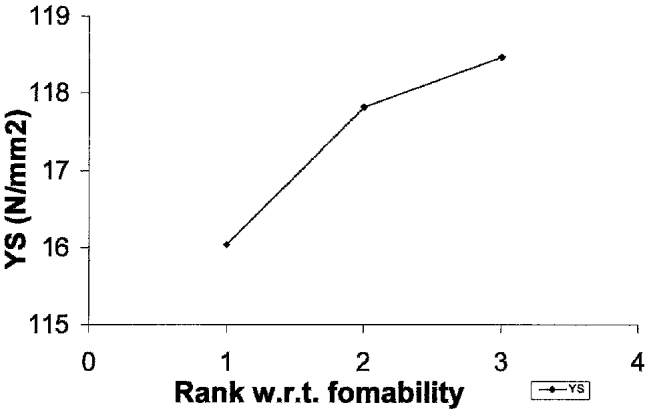

Fig. 12 Relative variation of YS for the best three heat treatments based on a low YS value (1 = 550/–17/24, 2 = 550/–17/8, 3 = 535/RT/1)

3.5 Average Plastic Strain Ratio (R-bar)

Because of the crystallographic texture sheet, metals generally exhibit significant anisotropy of mechanical properties. The normal anisotropy is assessed by the Lankford parameter or the plastic strain ratio, which characterizes the normal anisotropy of the sheet:

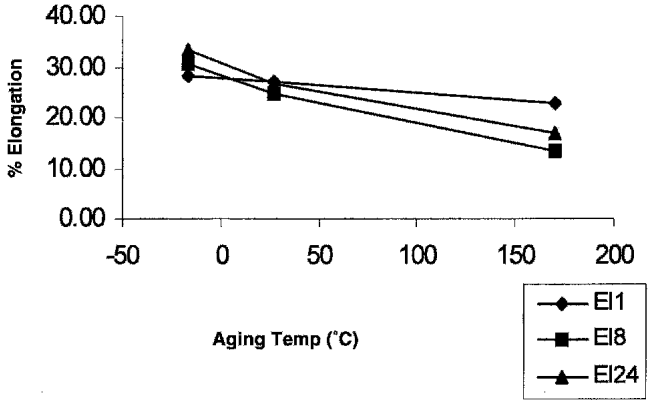

Fig. 13 Effect of aging temperature and time on percentage elongation in RD. Solutionizing temperature 550 °C

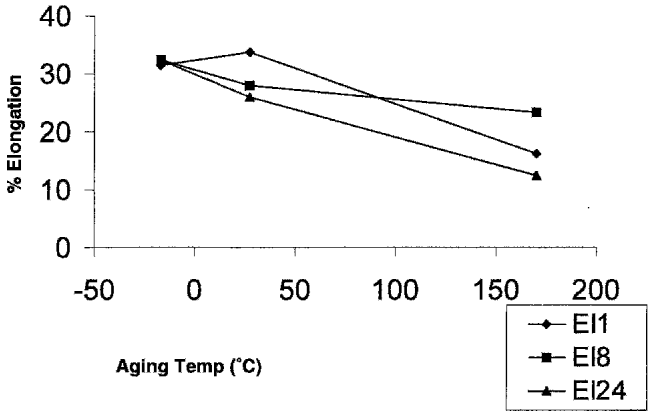

Fig. 14 Effect of aging temperature and time on percentage elongation at 45 degrees to the RD. Solutionizing temperature 550 °C

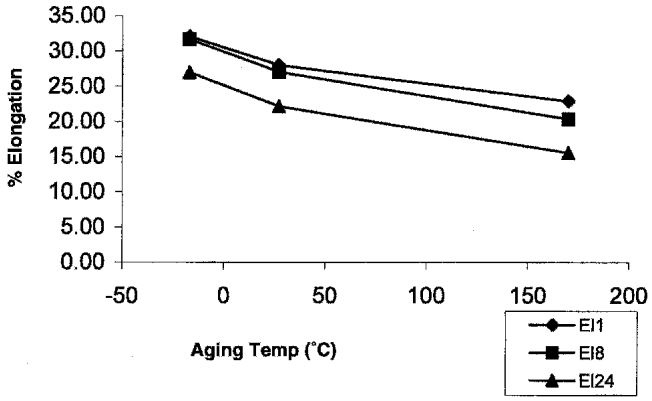

Fig. 15 Effect of aging temperature and time on percentage elongation at 45 degrees to the RD. Solutionizing temperature 520 °C

$$R = \varepsilon_W / \varepsilon_T \quad \text{(Eq 1)}$$

where ε_W and ε_T are the true strains in width and thickness directions, respectively, of the *R*-value specimen. The *R*-value characterizes resistance to thinning, and its average is calculated using standard definitions as:

$$\overline{R} = (R_0 + R_{90} + 2 \cdot R_{45})/4 \quad \text{(Eq 2)}$$

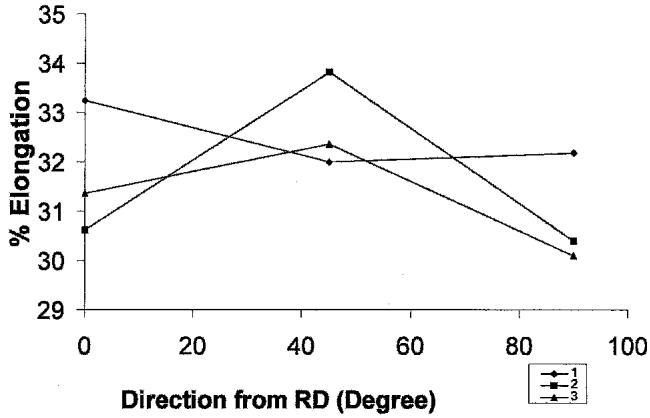

Fig. 16 Variation of percentage elongation with angle with respect to RD for the best three heat treatments (1 = 550/–17/24, 2 = 550/–17/8, 3 = 535/RT/1)

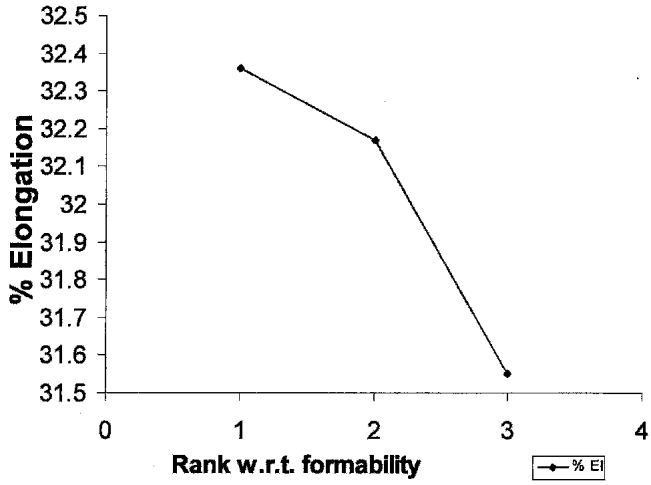

Fig. 17 Relative variation of percentage elongation for the best three heat treatments based on a high percentage elongation value (1 = 550/–17/24, 2 = 550/–17/8, 3 = 535/RT/1)

where R_0 is the plastic strain ratio evaluated at 0 degrees with respect to the RD.

The treatment 520/170/24 was found to be most suitable from the formability point of view. Figures 23 to 25 represent the maximum value of $\overline{R}$ for the best three heat treatment conditions. Figure 26 shows the comparison between values of $\overline{R}$ for best three conditions along the three different directions of anisotropy, while Fig. 27 is a similar comparison based on *R*-bar.

4. Discussion

Table 1 presents the best three heat treatments for various properties studied, and Table 2 shows the values of the material properties obtained from these heat treatments. It is clear from Table 1 that a single best heat treatment that will give the best of all properties studied cannot be found. A heat treatment for one property may not be the best for the other property from the formability point of view. Hence, for a given forming process a compromise must be made to obtain the most practicable heat treatment schedule.

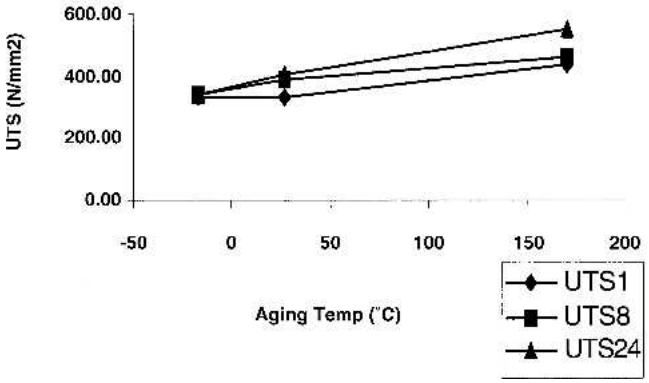

Fig. 18 Effect of aging temperature and time on UTS in RD. Solutionizing temperature 550 °C

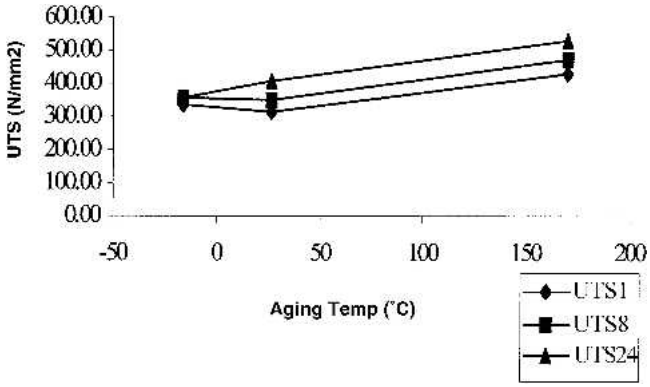

Fig. 19 Effect of aging temperature and time on UTS in RD. Solutionizing temperature 520 °C

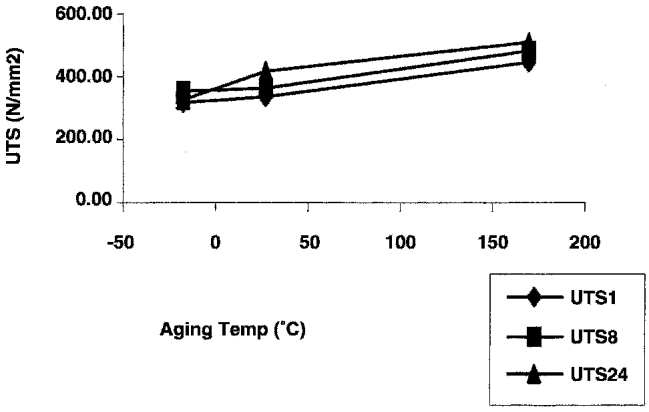

Fig. 20 Effect of aging temperature and time on UTS in RD. Solutionizing temperature 535 °C

This is achieved by determining the weighted performance index of the various heat treatments selected based on their good effect on the formability.

On inspecting Table 1, 10 independent heat treatments leading to high levels of formability indices emerge. The process of determining the best heat treatment for drawing and stretching is illustrated in Tables 2 to 5. Table 3 shows weights based on how well each heat treatment enhances the material properties so as to obtain greater formability, i.e., the treatment giving the lowest yield point gets 10 points and other treatments are

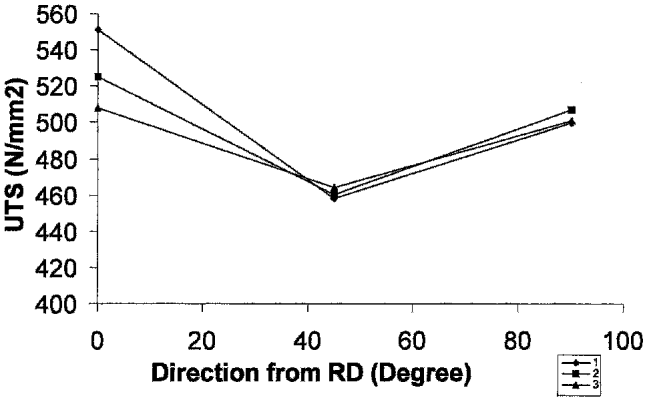

Fig. 21 Variation of UTS with angle with respect to RD for the best three heat treatments (1 = 550/170/24, 2 = 520/170/24, 3 = 535/170/24)

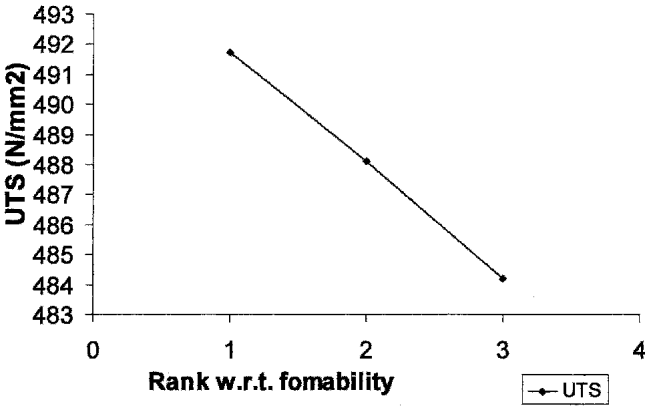

Fig. 22 Relative variation of UTS for the best three heat treatments based on a high UTS value (1 = 550/170/24, 2 = 520/170/24, 3 = 535/170/24)

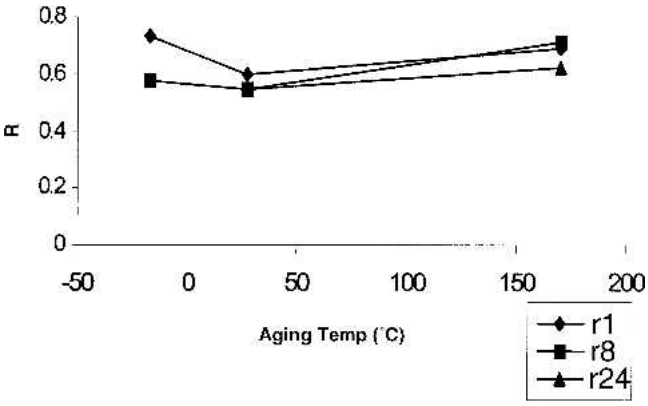

Fig. 23 Effect of aging temperature and time on R_{90}. Solutionizing temperature 520 °C

scaled linearly. Highest values of n, R, and percentage elongation all get 10 points. Finally, the relative weighted performance indices used to rank the heat treatments are evaluated in Tables 4 and 5 for deep drawing and stretch forming, respectively.

The best three heat treatments (based on higher weighted performance indices) lead to best formability. Of these, heat

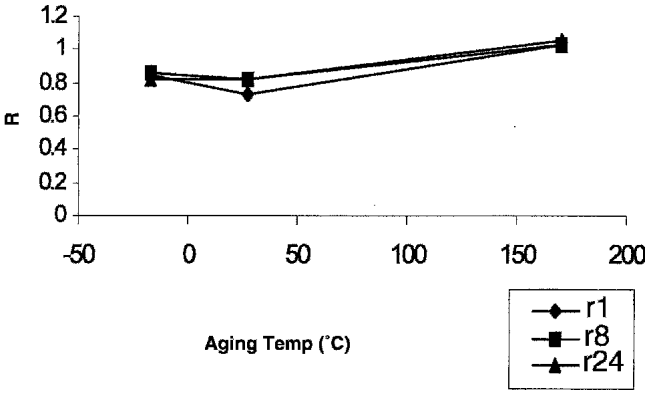

Fig. 24 Effect of aging temperature and time on R_{45}. Solutionizing temperature 550 °C

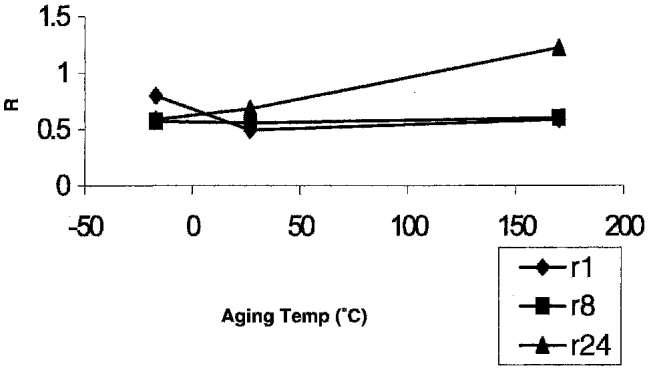

Fig. 25 Effect of aging temperature and time on R_0. Solutionizing temperature 550 °C

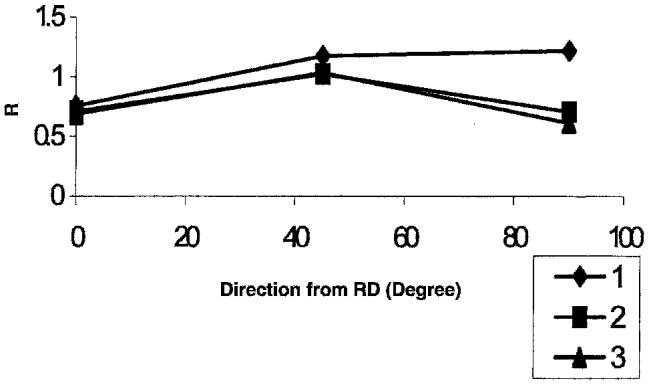

Fig. 26 Variation of R with angle with respect to RD for the best three treatments (1 = 520/170/24, 2 = 550/170/8, 3 = 550/170/1)

treatment 520/170/24 appears to be suitable for both drawing as well as stretching.

4.1 Deep Drawing

Based on sensitivity analysis of various material properties on the limiting draw ratio (LDR), one finds that normal anisotropy followed by the ductility of the material (given by percentage elongation) influence the LDR. Because n and YS do not influence the LDR significantly, they have been assigned a small weightage while calculating the weighted performance index.

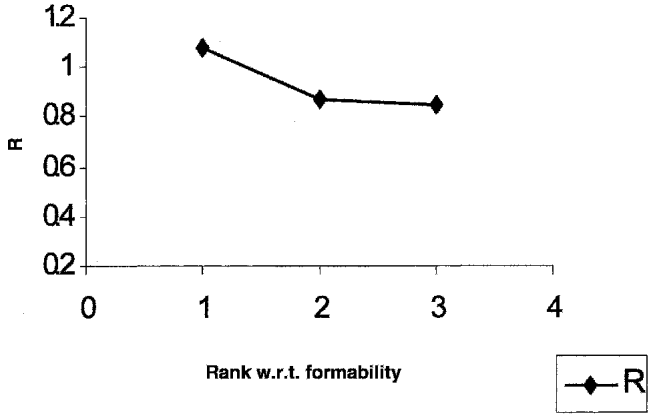

Fig. 27 Relative variation of R for the best three heat treatments based on a high R-value (1 = 520/170/24, 2 = 550/170/8, 3 = 550/170/1)

Table 1 Comparative presentation of best heat treatments (HT) for various properties

Property	HT ranked 1	HT ranked 2	HT ranked 3
n	520/170/24	550/170/24	535/170/24
YS	550/–17/24	550/–17/8	535/RT/1
UTS	550/170/24	520/170/24	535/170/24
% elongation	535/–17/24	550/RT/1	550/–17/24
R-value	520/170/24	550/170/8	550/170/1

Similarly, for the drawing load to be small, YS has the most significant influence followed by the R-value, a high value that reduces the flow stress. The significance of n is limited to the work hardening that takes place during deformation, causing a rise in the required load. Smaller YS as well as a high R-value reduces the wrinkling tendency. This is because the compressive circumferential stress, which causes wrinkling, decreases with a decrease in the drawing load, which in turn is proportional to flow stress. A high R-value promotes flow of the material in its plane, reducing the wrinkling tendency. Moreover, based on the tensile properties shown in Table 2, the weighted performance indices have been calculated and are shown in Table 4. It may be concluded that heat treatment 520/170/24 is the best compromise for the drawing process. Similarly, from the viewpoint of formability heat treatments 550/170/24 and 550/–17/24 may be ranked second and third, respectively.

4.2 Stretch Forming

Stretch forming is the process during which a sheet is clamped firmly on each end and stretched well beyond the elastic limit. From the viewpoint of formability in stretch forming a low resistance to thinning (as thinning is inevitable in stretching), uniform thinning and low load are important. Because values of n and YS are the major factors influencing thinning, they are assigned greater weights.

High-strain uniformity is ensured by a high value of n together with a low YS, high UTS and ductility in terms of percentage elongation. Forming load would be small with low YS and high UTS. The work hardening rate would affect the flow stress and hence the forming load.

Table 2 Values of various mechanical properties obtained to ensure high formability

Property	520/ 170/24	550/ −17/24	550/ 170/24	535/ −17/24	550/ −17/8	550/ RT/1	550/ 170/8	535/ 170/24	535/ RT/1	550/ 170/1
n	0.466	0.406	0.406	0.371	0.374	0.373	0.318	0.406	0.371	0.362
YS	116.04	117.82	118.47	125.29	117.82	122.12	284.31	369.55	117.47	253.54
UTS	491.74	488.11	484.20	313.92	308.89	317.78	440.64	484.20	313.00	414.53
% El.	32.36	32.17	31.67	32.40	30.06	32.17	20.49	15.83	29.78	17.98
R	1.084	0.698	0.793	0.631	0.721	0.653	0.868	0.686	0.653	0.844

Note: % El., % elongation

Table 3 Effect of heat treatments on the different mechanical properties obtained to ensure high formability (expressed on a 10-point scale)

Property	520/ 170/24	550/ −17/24	550/ 170/24	535/ −17/24	550/ −17/8	550/ RT/1	550/ 170/8	535/ 170/24	535/ RT/1	550/ 170/1
n	10	8.7	8.71	7.95	8.03	7.99	6.81	8.7	7.96	7.77
YS	9.85	10	9.8	9.26	9.88	9.5	4.08	3.14	9.85	4.58
UTS	9.93	8.43	10	6.38	6.28	6.46	9.85	9.85	6.37	8.96
% El.	9.93	9.93	9.77	10	9.28	9.99	6.32	4.88	9.19	5.55
R	10	6.44	7.31	5.83	6.66	6	8	6.33	6.03	7.79

Note: The heat treatment leading to a tensile property characterizing highest formability is assigned 10 points, and the others are scaled linearly. % El., % elongation

Table 4 Weighted performance indices for the different heat treatment for deep drawing

Property	520/ 170/24	550/ −17/24	550/ 170/24	535/ −17/24	550/ −17/8	550/ RT/1	550/ 170/8	535/ 170/24	535/ RT/1	550/ 170/1
n	1.30	1.13	1.13	1.03	1.04	1.04	0.88	1.13	1.03	1.01
YS	2.56	2.60	2.55	2.41	2.57	2.47	1.06	0.82	2.56	1.19
UTS	1.42	1.20	1.43	0.91	0.90	0.92	1.41	1.41	0.91	1.28
% El.	1.68	1.68	1.65	1.69	1.57	1.69	1.07	0.82	1.55	0.94
R	2.99	1.92	2.18	1.74	1.99	1.79	2.39	1.89	1.80	2.33
Total	9.94	8.53	8.94	7.78	8.06	7.91	6.81	6.07	7.85	6.74

Note: % El., % elongation

Table 5 Weighted performance indices for the different heat treatment for stretch forming

Property	520/ 170/24	550/ −17/24	550/ 170/24	535/ −17/24	550/ −17/8	550/ RT/1	550/ 170/8	535/ 170/24	535/ RT/1	550/ 170/1
n	3.03	2.64	2.64	2.41	2.44	2.42	2.07	2.64	2.41	2.36
YS	2.43	2.47	2.42	2.29	2.44	2.35	1.01	0.78	2.43	1.13
UTS	2.01	1.70	2.02	1.29	1.27	1.31	1.99	1.99	1.29	1.81
% El.	1.67	1.67	1.65	1.69	1.56	1.68	1.07	0.82	1.55	0.94
R	0.79	0.51	0.57	0.46	0.52	0.47	0.63	0.50	0.47	0.61
Total	9.94	9.00	9.31	8.14	8.24	8.23	6.76	6.73	8.16	6.85

Note: % El., % elongation

Table 6 Material properties used for fender and S-rail simulation of aluminum-lithium alloy and steel

Material	r_0	R_{45}	R_{90}	*R*-bar	*K*, MPa	*n*	YS, MPa	*E*, GPa	ν	ρ, g/mm^3
Al-Li alloy 550/170/1	0.687	1.036	0.616	0.844	1044.25	0.362	253.54	78	0.34	2.58×10^{-6}
EDD steel	1.88	1.4	1.79	1.618	590	0.249	290	206	0.33	7.8×10^{-6}

Calculations using the AHP, Tables 2 and 3, are summarized in Table 5. It may be concluded that heat treatment 520/170/24 appears to be the best compromise for good formability in stretch forming, whereas treatments 550/170/24 and 550/−17/24 rank second and third, respectively, from the stretch formability point of view.

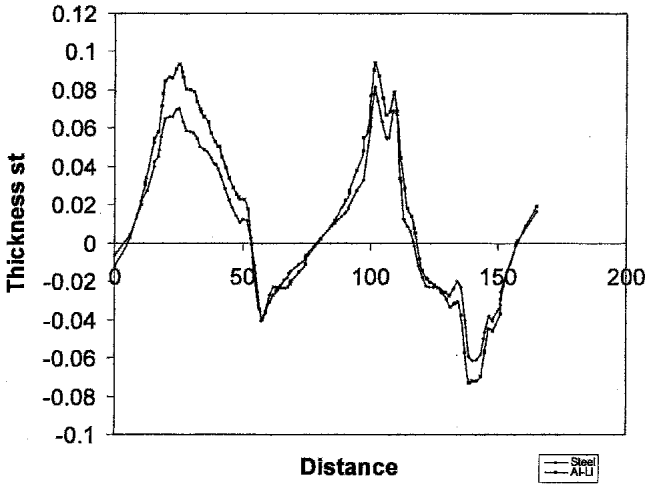

Fig. 28 Comparison of thickness strain for S-rail (aluminum-lithium versus steel)

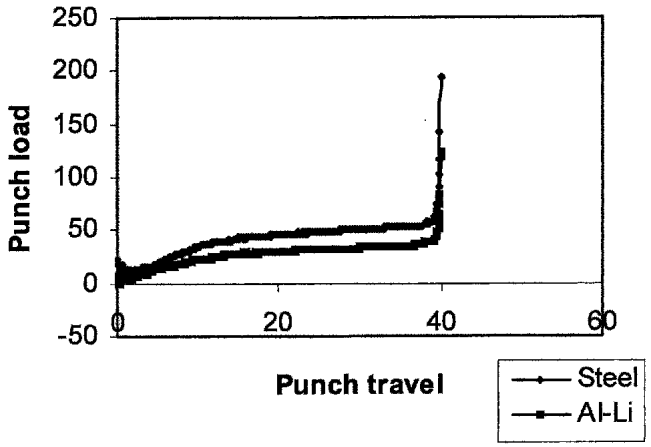

Fig. 29 Comparison of punch load for S-rail (aluminum-lithium versus steel)

5. Finite Element Simulations

After the identification of the best heat treatment, it was considered appropriate to compare the forming performance of the aluminum-lithium alloy with that of steel when forming two industrial parts, namely, an automobile fender and the S-rail (a structural member). The geometries were taken from NUMISHEET 2002 and NUMISHEET 99 benchmark problems and finite element method simulations performed (using PAMSTAMP2G software, Japan) for steel as well as the heat-treated aluminum-lithium alloy.

A relatively inferior heat treatment 550/170/1 was selected first for carrying out simulations. The purpose of selecting inferior heat treatment was to use a relatively conservative limit of formability in the simulation so that the selected heat treatment (despite minor variations in the heat treatment parameters) would still lead to a successful component. The forming performance of the heat-treated aluminum-lithium alloy sheet based on simulations was compared with that of the steel sheet.

The properties of the two materials used for simulation are given in Table 6. A comparison of thickness strain distribution and punch load for aluminum-lithium and steel for forming the

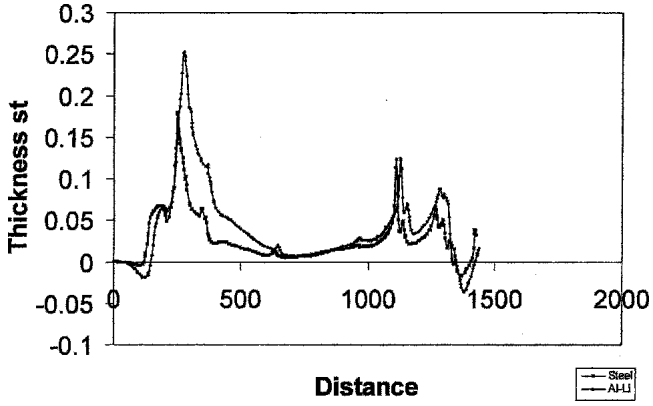

Fig. 30 Comparison of thickness strain for fender (aluminum-lithium versus steel)

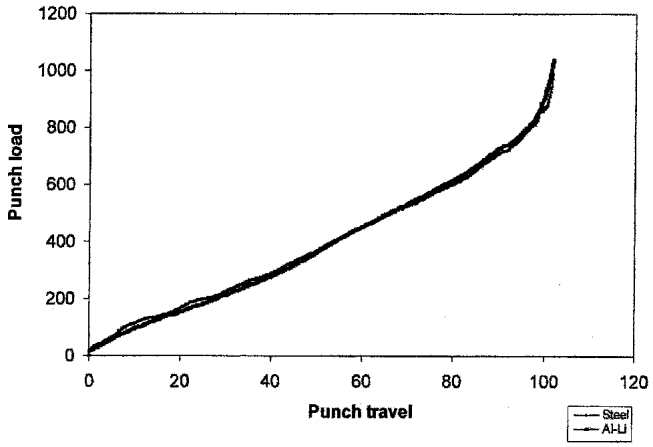

Fig. 31 Comparison of punch load for fender (aluminum-lithium versus steel)

S-rail are given in Fig. 28 and 29, respectively. A similar comparison is presented for the fender in Fig. 30 and 31. S-rail, being a structural member, requires higher stiffness and load-bearing capacity. The comparison between thickness strain distribution between steel and aluminum-lithium alloys can be seen in Fig. 28, where the aluminum-lithium alloy shows marginally more thinning. Interestingly both materials seem to need the same press capacity because of similar forming conditions. From Fig. 30, comparison of the thickness strain distribution for a fender shows that there is more thinning in case of the aluminum-lithium alloy, but part can be successfully formed to acceptable levels of thinning. The heat treatment selected for this analysis has a low weight factor. Still, a fender can be formed at this condition with the same processing conditions. The punch load for the aluminum-lithium alloy in Fig. 31 is similar to that of steel.

6. Economics of Weight Reduction: Future Projections

From the foregoing, it may be seen that from a technological point of view, aluminum-lithium alloys can substitute for steel very well. However, the economic standpoint must be examined, taking into account oil prices in the near future, oil con-

sumption, fuel efficiencies that may be achieved in the near future, and then weighing the savings made using the aluminum-lithium alloy against the higher cost of aluminum-lithium sheets. The analysis would have been complete if the cost escalation during manufacturing could have been taken into consideration, but in the absence of reliable representative data, a preliminary estimate of the savings has been presented in this paper.

The following calculation shows the relative advantage between steel and aluminum-lithium alloys forming a car body. Table 7 shows the weights of the various parts of a reference car made from steel (see also Ref 16). Table 8 presents a comparison between the savings from fuel efficiency compared with the higher cost of the aluminum-lithium material. The current costs of sheets of aluminum-lithium and steel have been obtained from Internet sources (Ref 17) and steel (Ref 18).

In the case of a car body, a weight reduction achieved through aluminum-lithium alloy can be justified in terms of fuel efficiency (saving in recurring fuel expense) against an increase in the cost of raw material. For instance, it is estimated that the cost of raw material would increase by $40.53 per body framing versus a saving of $279.21 per year on the recurring cost of fuel, assuming 25,000 km of driving each year (Ref 19). The extra one-time expense of body framing resulting from the higher cost of raw material, plus the manufacturing cost escalation (presently unknown) would be substantially offset by monetary benefits from fuel savings over a few years. Hence, actual manufacturing costs associated with aluminum-lithium alloy (which may require special manufacturing techniques or process improvements) has not been considered because of the unavailability of reliable data. This should be weighed against the savings on the recurring cost of fuel (which is expected to increase in the future as the availability of this natural resource is limited). Aluminum-lithium alloy therefore seems to hold promise as a future car body material.

Table 7 Reference car weight and detailed steel body framing weight

Car body weight	1340 kg	Detail about Front structure	67 kg
Details of body structure	478 kg	Part name	Weight in kg
Part name	Weight in kg	Front frame	4
Front structure	67	Lower longitudinal beams	12
Passenger cell	152	Upper longitudinal beams	6
Rear cell	59	Crash box	2
Exterior trim	33	Wheel houses	17
Bonnet	15	Fire wall	13
Doors	98	Fender	5
Boot lid	15	Miscellaneous	7
Miscellaneous	40		

Source: Ref 16

7. Conclusions

From the foregoing observations and discussions, the following inferences can be drawn:

- There is a negligible variation in the tensile properties at an aging temperature of –17 °C irrespective of aging time.
- There is a significant effect of heat treatments on the tensile properties.
- No single heat treatment could be identified to give the best set of tensile properties among those studied.
- From the view point of formability, the 520/170/24 treatment gives a high n value, 520/170/24 yields a high value of R, 535/–17/24 produces the maximum percentage elongation to failure, 550/–17/24 gives the least YS, and 550/170/24 produces high UTS.
- Based on the five tensile properties determined for each of the 27 heat treatments the 10 best treatments were subjected to analysis based on the weighted performance index in the context of deep drawing and stretch forming processes. The heat treatment 520/170/24 turns out to be the best compromise among these processes.
- Values of R were found to be maximum at 45 degrees to the RD, and hence ΔR is negative in all the cases.
- The results are consistent with the observation of high values of n and R at 170 °C aging temperature.
- The forming performances of aluminum-lithium alloys and steel, based on the thickness strain and punch load obtained from the simulation of a fender and S-rail, were found to be similar.
- The aluminum-lithium alloy shows adequate promise as an autobody material of the future because of rising oil prices and the weight advantage that aluminum-lithium alloy offers.

Table 8 Comparison of fuel consumption and weight reduction between steel and aluminum-lithium alloys

Sr. No	Weight of the reference car with steel material (Table 7)	1340 kg
1	Weight of body framing with steel (Table 7)	478 kg
2	Cost of steel (July 2004) (Ref 17)	$0.45/kg
3	Cost of raw material for steel body framing	$215.1
4	Weight of the car with aluminum-lithium	1032.05 kg
5	Cost of aluminum alloy (July 2004) (Ref 18)	$1.545/kg
6	Weight of body framing of aluminum = $478 \times (2.7 \times 10^6/7.8 \times 10^6)$	165.46 kg
7	Cost of raw material for aluminum alloy body framing	$255.63
8	Extra cost incurred for aluminum-lithium body framing (7–3)	$40.53
9	% weight reduction in car (1–4)/1	22.97%
10	Gasoline price (July 2004)	$35/barrel
11	Considering the steel reference car runs 3.5 gallons/h with the speed of 60 kmph fuel consumption/years fuel consumption per year (25,000 km running/year)	1457.5 gallon/year
12	Cost of fuel consumed/year for 25,000/km running of steel reference car	$1214.58/year
13	Saving on fuel cost (running cost/year) due to weight reduction considering 1% weight reduction leads to 1% fuel saving (Ref 19), therefore (1214.58×22.97)/100 is a cost saving/year for aluminum alloy	$279.21/year

Acknowledgment

The authors are grateful to the Aeronautical Research and Development Board of India for financial support.

References

1. K. Fukuo, A. Fujimura, M. Saito, K. Tsunoda, and S. Takiguchi, Development of the Ultra-Low-Fuel-Consumption Hybrid Car: INSIGHT, *JSAE Rev.,* Vol 22, 2001, p 95-103
2. D. Carle and G. Blount, The Suitability of Aluminum as an Alternative Material for Car Bodies, *Mater. Design,* Vol 20, 1999, p 267-272
3. D.V. Wilson, Aluminum Versus Steel in the Family Car on the Formability Factor, *J. Mechan. Working Technol.,* Vol 16, 1988, p 257-277
4. R. Shinnar, The Effect of the Energy Crisis on the Private Car in the U.S., *Transport. Res.,* Vol 9, 1975, p 87-95
5. D.L. Greene and K.G. Duleep, Costs and Benefits of Automotive Fuel Economy Improvement: A Partial Analysis, *Transport. Res.,* Vol 27a (No. 3), 1993, p 217-235
6. R.H. Essinhigh, Evaluation of Fuel Consumption Rates and Thermal Efficiency of Automobiles by Application of Furnace Analysis, *Transport. Res.,* Vol 8, 1974, p 457-464
7. M. Saito, S. Iwatsuki, K. Yasunaga, and K. Andoh, Development of Aluminum Body for the Most Fuel-Efficient Vehicle, *JSAE Rev.,* Vol 21, 2000, p 511-516
8. E. Romhanji, D. Mitlin, and V. Radmilovic, Deformation Pattern and Strain Hardening in a Highly Textured 8090 Al-Li Alloy Sheet, *J. Mater. Sci. Eng.,* Vol A291, 2000, p 160-167
9. R.K. Bird, D.L. Dicus, J.N. Fridlyander, and V.S. Sandler, Al-Li Alloy 1441 for Fuselage Application, *Seventh International Conference on Aluminum Alloys* (The Light Metals Centre at the University of Virginia, Charlottsville, Virginia), 2000, p 907-912
10. P.J.E. Bischler and J.W. Martin, Effect of Heat Treatment upon Tensile Strength and Fracture Properties of an Al-Li-Cu-Mg Alloy, *Proceedings of the Third International Aluminum-Lithium Conference* (Institute of Metals University of Oxford), 1985, p 220-233
11. P.S. Gilman, J.W. Brooks, and P.J. Bridges, High Temperature Tensile Properties of Mechanically Alloyed Al-Mg-Li Alloys, *Proceedings of the Third International Aluminum-Lithium Conference* (Institute of Metals University of Oxford), 1985, p 112-120
12. S.J. Harris, B. Noble, and K. Dinsdale, Effect of Composition and Heat Treatment on Strength and Fracture Characteristics of Al-Li-Mg Alloys, *Proceedings of the Second International Aluminum-Lithium Conference* (Metallurgical Society of AIME, Monteray, California), 1983, p 539-546
13. R.J. Kar, J.W. Bohlen, and G.R. Chennai, Correlation of Microstructures, Aging Treatments, and Properties of Al-Li-Cu-Mg-Zr I/M and P/M Alloys, *Proceedings of the Second International Aluminum-Lithium Conference* (Metallurgical Society of AIME, Monteray, California), 1983, p 255-285
14. J. White, W.S. Miller, I.G. Palmer, R. Davis, and T.S. Saini, Effect of Precipitation on Mechanical Properties of Al-Li-Cu-Mg-Zr Alloy, *Proceedings of the Third International Aluminum-Lithium Conference* (Institute of Metals University of Oxford), 1985, p 530-538
15. M.L. Bairwa and P.P. Date, Effect of Heat Treatments on Tensile Properties of Al-Li Alloys, *Proceedings of International Conference AMPT2003* (Dublin City University, Dublin), 2003, p 115-118
16. http://www.eaa.net/downloads/Alumax%20A%20%20Final%20report.pdf
17. http://economictimes.indiatimes.com/articleshow/msid-754330,prtpage-1.cms
18. http://www.lme.co.uk/dataprices_monthlyvolumes.asp
19. R.J. Pallett and R.J. Lark, The Use of Tailored Blanks in the Manufacture of Construction Components, *J. Mater. Processing Technol.,* Vol 117, (No. 1-2), 2001, p 249-254